Article

Chitosan Membranes for Direct Methanol Fuel Cell Applications

Fulufhelo Nemavhola * , Livhuwani Modau , Rudzani Sigwadi , Mouhumi Mokrani

Posted Date: 17 July 2023

doi: 10.20944/preprints202307.1088.v1

Keywords: Chitosan; Fuel Cell; Water Uptake; Proton Conductivity; Silica, Sulfonated doi:10.20944/preprints202307.1088.v1

Article

Chitosan Membranes for Direct Methanol Fuel Cell Applications

Livhuwani Modau [1,*], Rudzani Sigwadi [1], Mouhumi Mokran [1] and Fulufhelo Nemavhola [2]

[1] Department of Chemical Engineering, University of South Africa, Private Bag X6, Florida, 1710, South Africa
[2] Department of Mechanical Engineering, Faculty of Engineering and the Built Environment, Durban University of Technology, Durban, South Africa, 4000
* Correspondence: fulufhelon1@dut.ac.za

Abstract: The purpose of this study is to identify the steps involved in fabricating silica/chitosan composite membranes and their suitability in fuel cell application. It also intends to identify the physical characteristics of chitosan composite membranes, including their degree of water absorption, proton conductivity, methanol permeability, and functional groups. In this investigation, composite membranes were fabricated using the solution casting method with chitosan content of 5 g and silica variations dosage of 2 % and 4% while stirring at a constant speed for 2h. According to the findings, the analysis of composite membranes produced chitosan membranes that were successfully modified with silica. The optimum membrane was found to be 4 % s-SiO_2 from the Sol-gel method with composite membrane's optimal condition of 0.234 cm/s proton conductivity, water uptake of 56.21%, and reduced methanol permeability of 0.99×10^{-7} cm^2/s in the first 30 minutes and 3.31 $\times 10^{-7}$ in the last 150 minutes. Maintaining lower water uptake capacity at higher silica content is still a challenge that needs to be addressed. In conclusion, the fabricated membranes showed exceptional results in terms of proton conductivity and methanol permeability.

Keywords: chitosan; fuel cell; water uptake; proton conductivity; silica; sulfonated

1. Introduction

The increasing scarcity of fossil fuels has highlighted the need for alternative energy sources [1–3]. Fuel cells are regarded as a promising technology that can be utilized to address this issue. They are widely used in the context of carbon neutralization and carbon peaking. Fuel cells can also work well with other clean energy sources such as methanol. Depending on the electrolyte's type, the fuel cell can be categorized into different types such as proton exchange membrane fuel cells, also known as PEMFCs, solid oxide fuel cells (SOFCs), Alkali fuel cells (AFCs), molten carbonate fuel cells (MCFCs) fuel cells [4–7]. The PEMFC is one of the most widely used energy techniques in the world due to its high energy conversion efficiency and lack of pollution [8,9]. Direct methanol fuel cell (DMFC) is a promising technology that is expected to revolutionize the way we produce and use electricity [4,8]. DMFCs have attracted widespread attention due to their unique attributes, such as their low emission, easy liquid fuel storage, and high energy density [10,11]. DMFCs are based on liquid-fuel technology and utilize direct methanol as their fuel for electricity generation [12]. They are market leaders in the field and are commonly utilized in mobile and off-grid power applications [13,14]. Polymer membranes are the main components of direct methanol fuel cells [15–17]. DMFCs must be designed to provide high-ion exchange capacity and low-water uptake. They should also have good proton conductivity and a long-life span [18,19]. The high proton conductivity of PEM ensures that it can conduct protons efficiently from the anode to the cathode. Its robust fuel barrier helps prevent degradation or even the termination of fuel cell performance [7]. Its good mechanical properties ensure that it operates in both wet and dry environments. Today's membranes are made from perflurosulphonic acids, which are commonly referred to as Nafion. Unfortunately, Nafion has drawbacks such as high methanol permeability and high cost which also contribute to its application in the fuel cell [19,20]. Natural and low-cost abundant chitosan-based polymers can be utilized as an alternative in fuel cells. However, due to their high hydrophilic nature and low proton conductivity, they are not ideal for DMFC applications [4]. The biopolymer Chitosan is made from chitin, which is found in the shells of insects and crustaceans. With the help of hygroscopic oxide fillers such as silica (SiO_2), Titanium dioxide (TiO_2), and Zirconium Oxide (ZrO_2), they can achieve good membrane properties such as high proton conductivity, low water uptake, high membrane selectivity, and methanol permeability [21,22]. Several studies have also shown that chitosan membranes made with pure/sulfonated silica exhibited better proton conductivity and water uptake than those made without this modification. Chitosan membranes are commonly modified with silica nanoparticles to enhance their mechanical strength, stability, and barrier properties. The addition of silica can improve the overall performance of the membrane by reducing the permeability of certain molecules, including methanol [21,22]. The chitosan structure has two major groups: the amino and the hydroxy groups, which makes it easy to modify. Depending on the modification process, chitosan can undergo physical and chemical transformations [23]. Chemical modification can be performed on either the amino or the hydroxy groups depending on the reaction [23]. Although the primary group of chitosan reacts actively to the amino group, it is less reactive than the secondary group. When a chemical modification is carried out on the amino group, it will be labelled as N, while it will be O modified on the other side. Physical methods can be utilized to modify chitosan, such as mechanical grinding, ultrasonic treatment, and ionizing radiation [24]. DMFC utilizes different types of membranes based on their morphological attributes. These include thick, thin, layered, porous, and pore-filled membranes [25]. Although the properties of chitosan can be modified to improve its suitability for fuel cells, membrane morphology can still have a significant impact on its performance. For example, DMFC's thin membranes are prone to experiencing high methanol crossover when compared to thick ones.

2. Experiment

2.1. Materials

Chitosan flakes, Medium molecular weight, (Merck), Tetraethyl orthosilicate, $Si(OC_2H_5)_4$, 98%, (Merck), Ammonia, NH_3, 25%, (Merck), Acetic acid, CH_3COOH, 99%, (Merck), Sodium hydroxide, NaOH, (Merck), Ethanol, C_2H_5OH, 99.9%, (Merck), Methanol, CH_3OH, 99.9% (Merck), Sodium chloride, NaCl, (Merck), Hydrochloric acid, HCl, 37%, (Merck), Sulfuric acid, H_2SO_4, 99%, (Merck), Taurine, $C_2H_7NO_3S$, 99%, (Merck)

2.2. Synthesises of SiO_2 Nanoparticles

(i) Sol-gel Process

The process for producing silica particles using tetraethyl orthosilicate involves the condensation and hydrolysis of TEOS. Various substances, such as 200 ml of ethanol, 80 ml of TEOS, and ammonia, were stirred at varying temperatures for around 30 minutes. A substance resembling a sol-gel was then dried at a rate of 100 ℃ for a single day. The silica particles were then catalysed to remove impurities by calcinating them at a rate of 600 ℃ degrees for 2 h.

(ii) Stober Process

The precursor for silica was TEOS during the Stober process, which involved the addition of ammonia, water, and ethanol. The mixture, which was then centrifuged for over 30 minutes, was then purified using a gasifier. The white solid materials, which were dried at a rate of 100 ℃ for 24 hours, were then subjected to a similar process as those of Sol-gel.

2.3. Sulfonation Process

Sulfuric acid was used to prepare silica nanoparticles. These particles were sulfonated to improve their proton conductivity. The process used for producing sulfonated silica nanoparticles for the Sol-gel and Stober processes was the same. In a mixing process, 10 g of silica particles were mixed with 5 ml of sulfuric acid and 200 ml of methanol. At 1500 rpm, the mixture was vigorously stirred. It was then subjected to a continuous centrifuge for about 31 minutes.

2.4. Fabrication of Composite Membranes (Casting Method)

Chitosan flakes were used to make chitosan membranes. The casting technique was used to create the membranes. Chitosan flakes weighing 5g were added to a 2% v/v acetic acid solution and agitated for an hour. DMSO, taurine, and silica particles (2%, and 4%). The gel solution was dried at 70 °C for 5 h. The acquired dried membrane was cross-linked with 2M sulfuric acid for 30 minutes before being submerged in NaOH. The membrane surface was then cleansed with deionized water to remove any surplus acid. Sulfonated silica-chitosan membranes were also processed in this manner.

3. Characterization Techniques

3.1. Water uptake

The water uptake ratio is a measure of how much water can be absorbed by a membrane. This is very important in the design and construction of fuel cell membranes. The water uptake rate is also a factor that contributes to the membrane's swelling capacity. Cell efficiency can be affected by high water uptake. The difference in the membranes' mass between those that are dehydrated and hydrated is used to determine how much water they take up. The mass of a wet membrane can be measured after it has been soaked for a couple of hours, while that of a dry one will be assessed before it is exposed to water. Water uptake is calculated as follows:

$$\text{Water (\%)} = \left(\frac{Gw-GD}{GD}\right)\times 100\% \qquad (1)$$

where G_W is described as the weight of wet membranes and G_D is the Dry membrane’s weight.

3.2. Ion Exchange Capacity (IEC)

The ion exchange capacity was measured using the method used by Sigwadi et al., (2009). Membranes that were in the acidic form were put in NaCl solution for 24 h for Na^+ to interchange H^+ ions. The H^+ ion that was released was titrated with a solution of sodium hydroxide using a phenolphthalein indicator. The membrane film was then dipped in a 20 ml aqueous solution of 2M sodium chloride to allow the substitution of protons with Na^+ ions. The protons that were released were titrated with 0.01 M sodium chloride solution until it reaches a pH balance. Ion exchange capacity was calculated as follows:

$$\text{IEC} = \frac{VNaOH * CNaOH}{Mdry} \qquad (2)$$

where IEC is the ion exchange capacity of the membrane, C_{NaOH} is – Concentration of NaOH in mol/l, V_{NaOH} is- Volume of NaOH that will be used to neutralize H+ in ml, Mdry is- Mass of dry membrane in g.

3.3. Methanol Permeability

Membrane permeability to methanol was determined at room temperature by a two-compartment diffusion cell having the membrane in-between. Both A and B cell compartments were loaded with the same amount of Methanol fuel and water respectively. Both sides of the cell were stirred. Permeability values were calculated as follows:

$$\text{P} = \frac{L}{A}\times\frac{V_b}{C_a}\times\frac{\Delta C}{\Delta t} \qquad (3)$$

P-Permeability-Thickness of the membrane, A-Area available for diffusion in the membrane-Volume of receiving compartment, Ca is the Concentration of sample in component A, ΔC is the change in methanol concentration, Δt is the permeation time.

3.4. Brunauer-Emmett-Teller (BET) measurements

The BET analysis was carried out using the Micrometric 3-Flex system. After the gas has been purged, a dry sample will be cooled down to around 77 K using liquid nitrogen. The inert gas will then adhere to the surface of the sample and lower the pressure inside the analysis chamber (' Walton and Snurr, 2007; Peyrovi and Parizi, 2022). Then the adsorption isotherm of the experiment was used to determine the surface area of the samples. All samples were degassed under a pressure of around 3 x 10^{-5} mbar. Particles size can be determined using the following equation:

$$S= \frac{6}{\rho D_{BET}} \times 10^3 \qquad (4)$$

ρ-denote the theoretical density of the material, and $D_{BET} -$ denote the size of the particle in nm

3.5. X-ray Powder Diffraction Analysis (XRD)

XRD includes structures, preferred crystal orientations (texture), and additional structural elements such as crystallinity, average grain size, crystal flaws, and strain. The constructive interference of a monochromatic beam of X-rays dispersed at precise angles from each pair of a sample's lattice planes results in the formation of X-ray diffraction peaks. The arrangement of atoms within the lattice affects peak intensities. As a result, each material's periodic atomic configurations are identified by its X-ray diffraction peaks. According to Bragg's law, constructive interference (and a diffracted ray) take place when incident rays come into contact with a sample [28]. Braggs's laws equation

$$n\lambda = 2d\sin\theta \qquad (5)$$

This theory relates the diffraction angle and lattice spacing of a crystalline sample to the electromagnetic radiation spectrum. After that, the diffracted X-rays are detected, examined, and counted. Due to the non-uniform dispersion of the powdered material, scanning the sample at a range of 2 should reveal all possible lattice diffraction orientations. The chemical can be recognized by converting the diffraction peaks to d-spacings even though eac`h material has a unique set of d-spacings. This is typically accomplished by comparing d-spacings to recognized reference patterns.

4. Results and Discussion

4.1. Fourier Transform Infrared for chitosan membranes

FTIR spectra were used to analyse the SiO_2 creation in the hybrid chitosan-silica composite. The spectra were obtained for both the modified and pure chitosan membranes. The analysis of the membranes using FTIR is in Figure 1. revealed that the membranes exhibited a peak between 3370 and 3250 cm $^{-1}$. This peak represents the presence of the N-H group that had an overlapping relationship with the O-H group [29]. The peak was shifted in the composition of modified chitosan membranes from 3331 cm^{-1} to (a and b) 3338 cm^{-1}, (c) 3294 cm^{-1}, and (d) 3333 cm^{-1} of Figure 1A, and in Figure 1B it shifted to (a) 3343 cm^{-1}, (b) 3379 cm^{-1}, (c) 3409 cm^{-1} and (d) 3428 cm^{-1}. The shift in the peak shows that the interaction between the N-H of chitosan and silica's O-H groups is occurring. The peaks at 2846 cm^{-1} and 2921 cm^{-1} are respectively related to the vibrations produced by the C-N and C-H stretching [30]. The CS and the CS/(SiO_2/s-SiO_2) membrane's amino group's N-H bond deformation is at 1518 cm^{-1}. The absorption bands found on the Stober (1020 cm^{-1}), and Sol-gel (1014 cm^{-1}) membranes are believed to be caused by Si-O-S vibration. On the other hand, the absorption bands found on the 873 and 862 cm-^{1} membranes were attributed to Si-OH (Diaconu et al., 2010). Although the spectra did not show a new functional group, the membranes made by sol-gel exhibited high-intensity peaks, which is a result of their interaction with chitosan and silica.

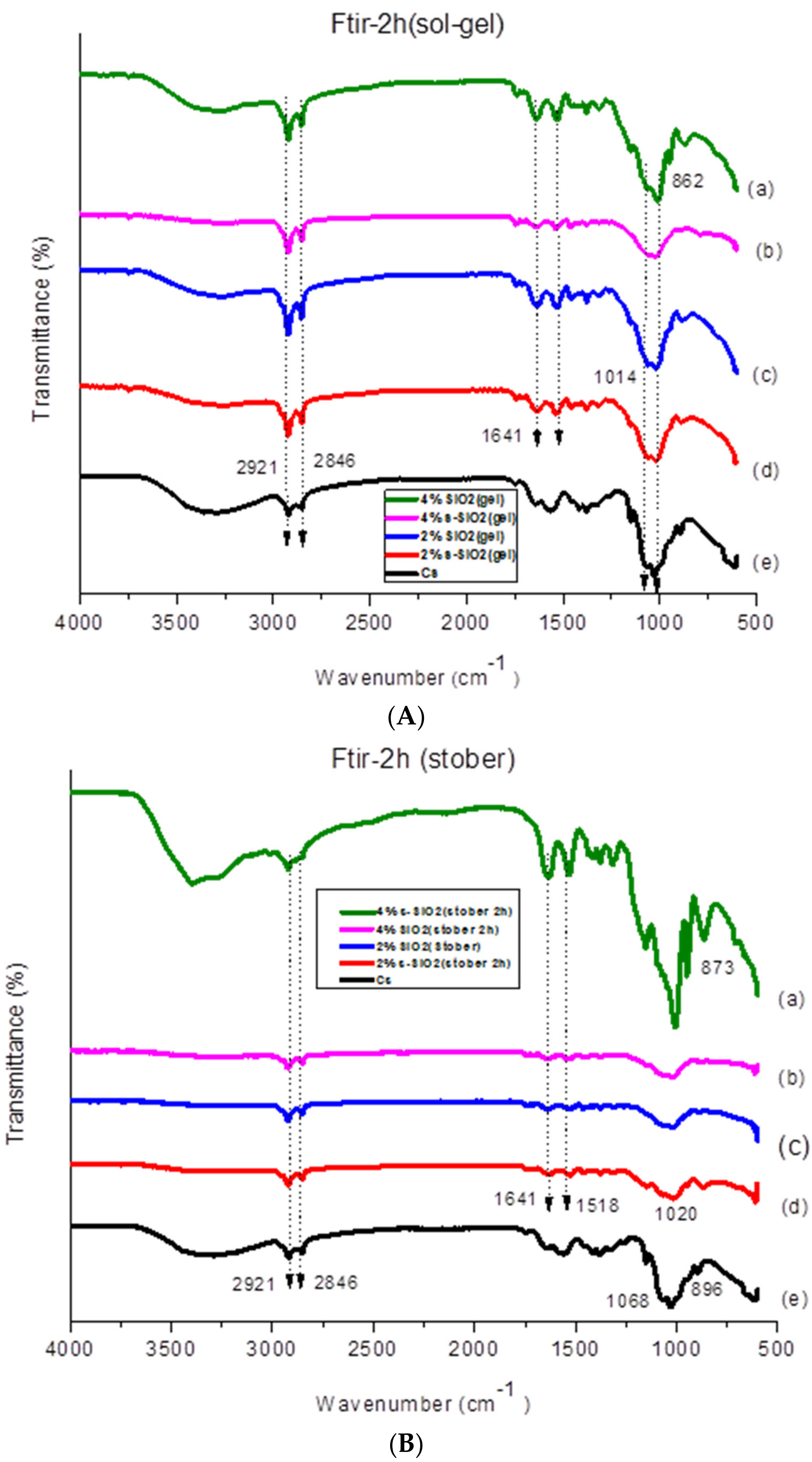

Figure 1. (**A**) FTIR of (a) 4% s-SiO_2/Cs (b) 4% SiO_2/Cs (c) 2% SiO_2/Cs (d) 2% s-SiO_2/Cs (e) Cs—**Sol-gel (2h)**. (**B**) FTIR of (a) 4% s-SiO_2/Cs (b) 4% SiO_2/Cs (c) 2% SiO_2/Cs (d) 2% s-SiO_2/Cs (e) Cs—**(Stober 2h)**.

4.2. X-ray Diffraction of chitosan membranes

The interactions between the chitosan molecules' intramolecular and intermolecular components contribute to their crystallinity. The XRD method was used to determine the SiO_2's impact on the crystallinity of CS. Figure 2 shows the XRD analysis of various types of membranes, including 2% s-SiO_2 and 4% s-SiO_2. The chitosan membrane exhibits semi-crystalline characteristics at 19°. The modified membranes exhibited an amorphous structure with different angles of refraction, such as 19.78, 20.29, 21,26, and 21.35 degrees. The crystallinity loss experienced during the process of modification can be seen in Figure 2. The figure displays the decrease in the modified chitosan membranes' crystallinity peak. modified membranes exhibited an amorphous structure and the addition of silica fragments containing sulfuric acid resulted in a reduction in total crystallinity.

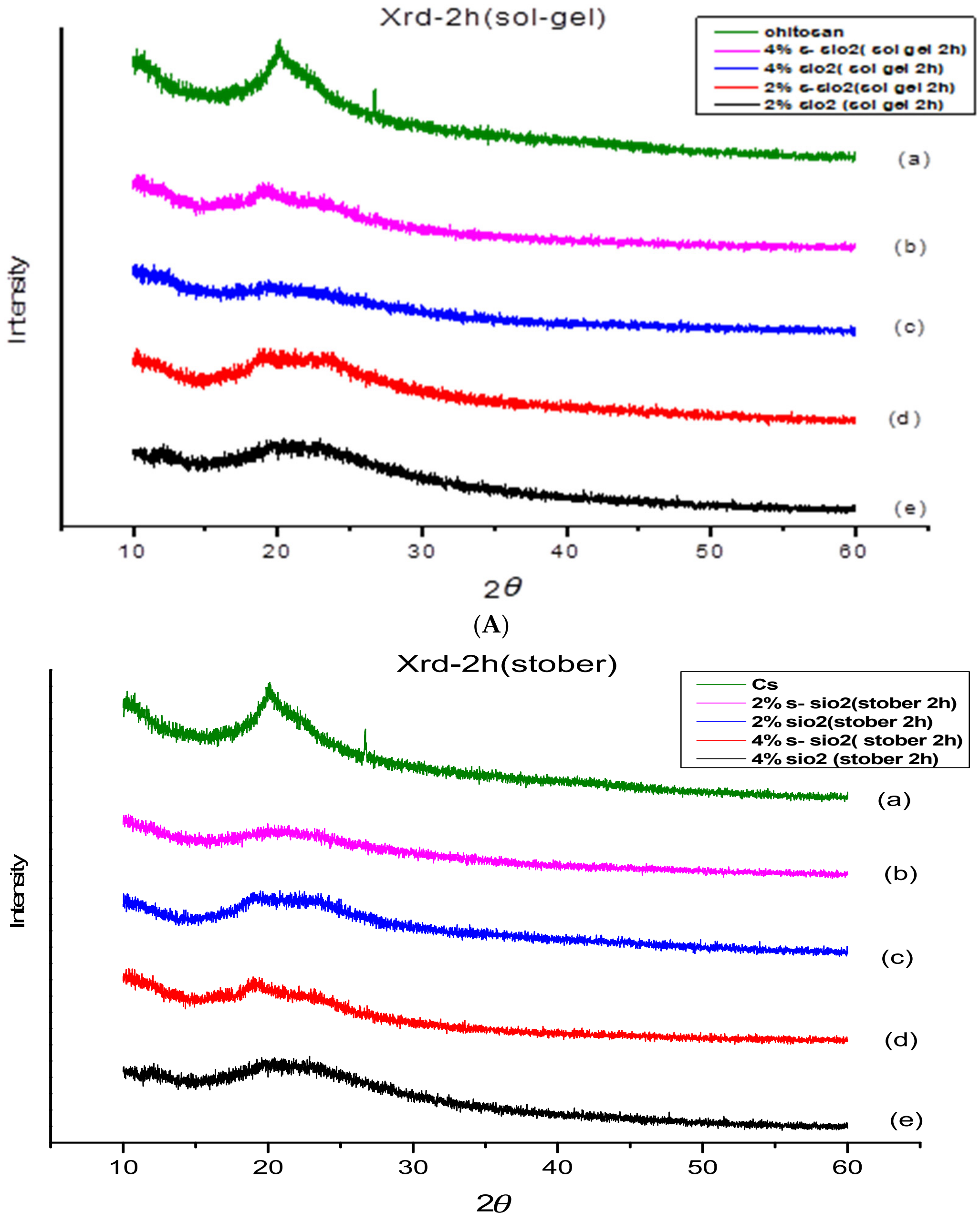

(**A**)

(**B**)

Figure 2. (**A**) XRD of (a) Cs (b) 4% s-SiO_2/Cs (c) 4% SiO_2/Cs (d) 2% s-SiO_2/Cs (e) 2% SiO_2/Cs—**Sol gel (2h)**. (**B**) XRD of (a) 2% SiO_2/Cs (b) 2% s-SiO_2/Cs (c) 4% SiO_2/Cs (d) 4% s-SiO_2/Cs (e) Cs—**(Stober 2h)**.

4.3. SEM of chitosan membranes

Figure 3 indicate the morphologies of the chitosan membranes. The changes in Chitosan's morphology were observed using SEM. These transformations were observed before and after SiO_2 modification. The image in Figure 3(Aa) shows a smooth and complex surface that does not have any visible pores on it. The results support the findings of a study conducted by Riek and colleagues in 2017, who discovered that the chitosan membrane has uniform and homogenous flat surfaces and a consistent thickness. The incorporation of silica in chitosan membranes in Figure 3(Ab–Ae) roughened their surface. A lot of silica nanoparticles are visible in membranes a and b while in membranes c and d little amount of silica was detected in Figure 3A. This is due to the number of silica nanoparticles that were added to the membranes as membrane a and b has high silica content compared to those of c and d. It is evident that although silica nanoparticles were dispersed it was not evenly distributed in the polymer matrix of all the membrane. It also appears that the dispersed nanoparticles form aggregates and the more amount of silica added the higher the number of agglomerated silica nanoparticles. The high energy level of silica particles causes silica agglomeration. However, modification of silica with sulphur seems to reduce this agglomeration since membranes b and e have lower agglomerates compared with those of their unmodified silica membranes.

Physical morphologies of membranes with silica synthesized through Stober are indicated in Figure 3B. The SEM images indicate membranes with dense morphologies and hard surfaces. Membranes with silica from Stober have similar morphologies to those of Sol-gel. However, membrane (a) (2% SiO_2) in Figure 3B has lumps on it which may have developed during the drying process, but these lumps are not visible in other membranes. When looking at membrane c of Figure 3B it can be observed that it has a better distribution of silica on its surface, but agglomeration is also visible. The agglomeration phenomena have occurred in all of the fabricated membranes (Sol-gel and Stober) and membranes with silica synthesized though Stober have more agglomerates in their surface compared to those of Sol-gel. The challenge is still to synthesize silica particles that will form little to no agglomerates for modification of chitosan modification.

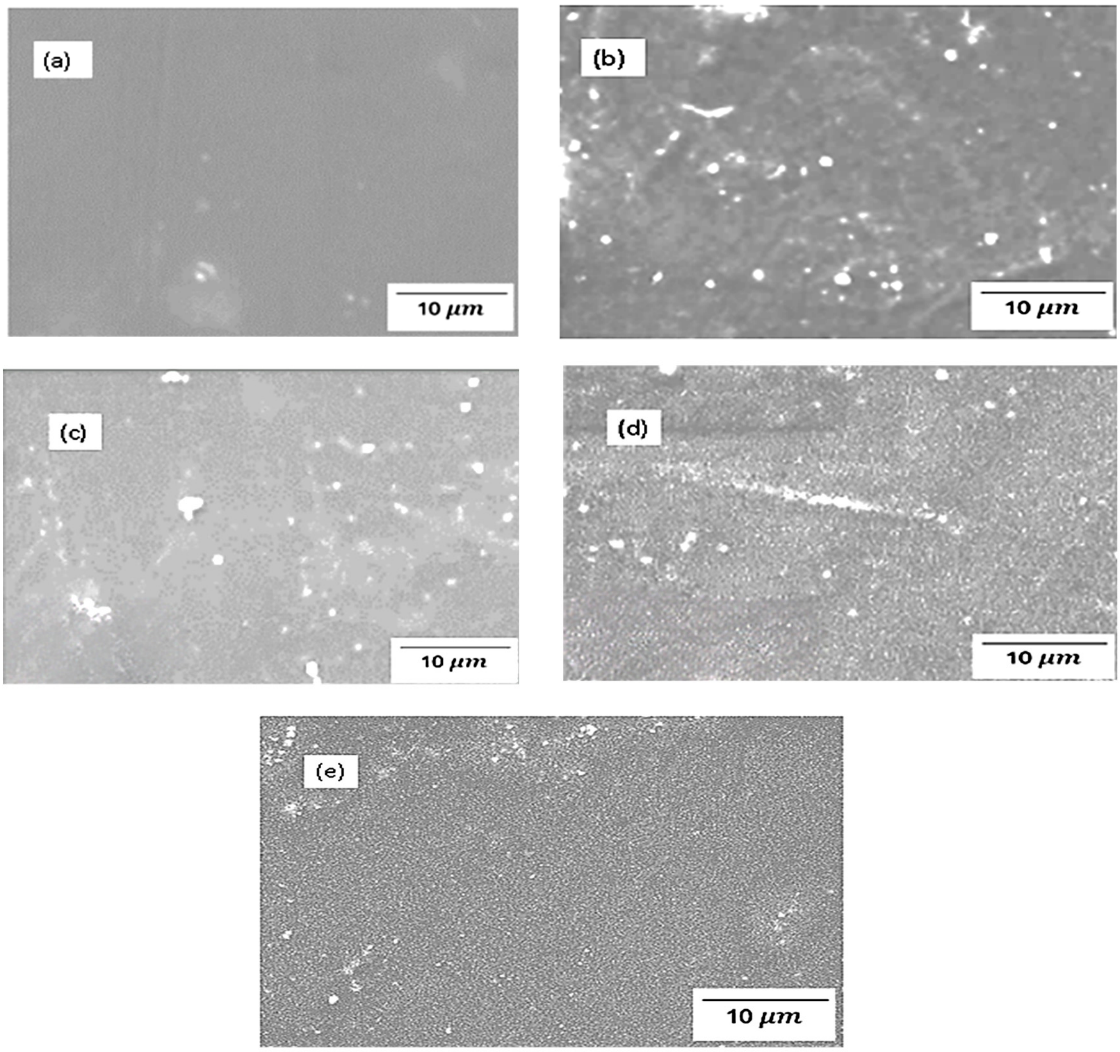

(**A**)

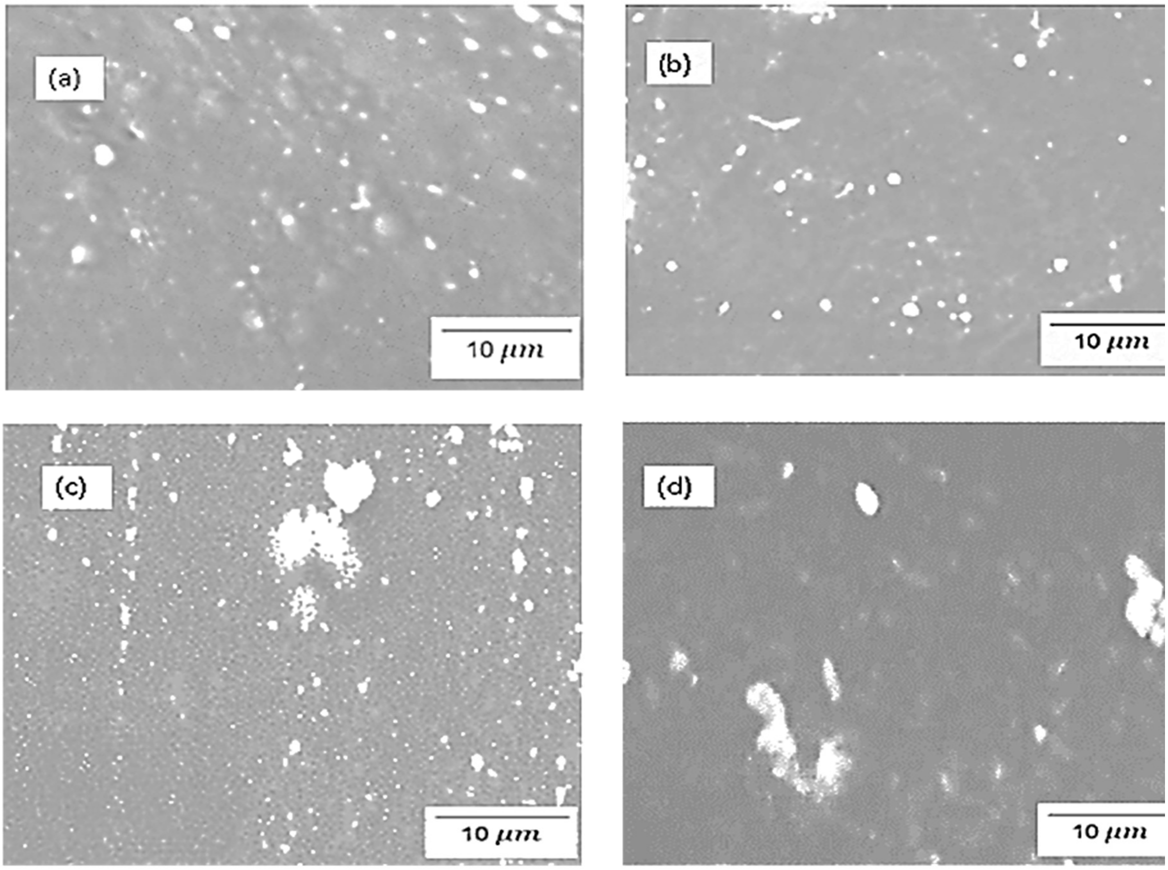

(**B**)

Figure 3. (**A**) SEM of (a) Cs (b) 4% s-SiO_2/Cs (c) 4% SiO_2/Cs (d) 2% s-SiO_2 /Cs (e) 2% SiO_2/Cs **Sol-gel (2h)**. (**B**) SEM of (a)2% s-SiO_2/Cs (b) 2% SiO_2/Cs (c) 4% s-SiO_2/Cs (d) 4% SiO_2/Cs **Stober (2h)**.

4.4. Water uptake of chitosan membranes

(i) Effect of Silica Content on Water Uptake

The membrane water uptake is a vital part of its physical properties. The water uptake of chitosan membranes as a function of silica (SiO_2/s-SiO_2) is shown in Figure 4A. The chitosan contains different silica contents of 2 % and 4 %. It can be seen that the incorporation of silica into the chitosan matrix suppresses the water absorption of the membrane uptake by 22 % on 2% SiO_2/Cs, however, adding more silica content to the membrane resulted in an increase in water uptake as membranes containing 4% SiO_2 has higher water uptake of 45.34 % and 47.98% whilst that of the corresponding 4% s-SiO_2 are 51.97% and 56.21% Stober and Sol-gel respectively. The increase in water uptake at higher silica levels can be attributed to silica hygroscopic affinity and bonding interaction between the silanol group and chitosan amine, acetyl, and silanol groups interacting more strongly increasing membrane hydrophilicity [31]. The highest water uptake is 56.21 % belonging to the 4% s-SiO2 membrane. Higher values in s-SiO_2 membranes are due to the presence of sulfonic acid groups on the surface of the silica particles, which can interact with water molecules and promote their uptake. These findings indicate that making use of chitosan modified with a small quantity of silica can lead to significant improvements in the membranes' water uptake capacities, potentially affecting a wide range of applications.

(ii) Effect of Temperature on Water Uptake

Figure 4B represents the effect of temperature on the water uptake of chitosan membranes. The temperature can influence how the chitosan and silica composites will expand. This is because higher temperatures can cause the molecules of solvent to expand into the matrix. The processing conditions and composition of the composite will determine how much swelling will occur. As shown above, in Figure 4B, the membranes show an increase in water uptake when the temperature rises from 40 ℃ to 60 ℃, however, the water uptake on modified membranes was lower than that of pure chitosan recorded to be 60%. Modified membranes have uptake between 53.26 ℃-68.92 ℃ (Sol-gel) and those of Stober are 53.25 ℃- 69.39 ℃ at 40 ℃ - 60 ℃. The increase is due to membrane water diffusivity, chain mobility, and membrane-free volume. However, the 4% s-SiO_2 sol-gel membrane doesn't show a significant change from 40 and 60 ℃ as its water uptake is 65.17 % and 65.35 % at 40 ℃ and 60 ℃ respectively. The minimal water uptake rate on the 4% s-SiO_2 membrane can be attributed to the chitosan and silica interaction as well as the lack of free void volume, which enables the membranes to endure high temperatures. It can be said that membranes with silica synthesized through sol-gel have high water compared to those of Stober with s-SiO_2/Cs membranes having the highest water uptake. This can reduce membrane application if the membranes become spongy reducing their life span. In conclusion, Stober membranes' low water uptake is an ideal property for fuel cell applications. Also, the minimal water uptake can improve their durability.

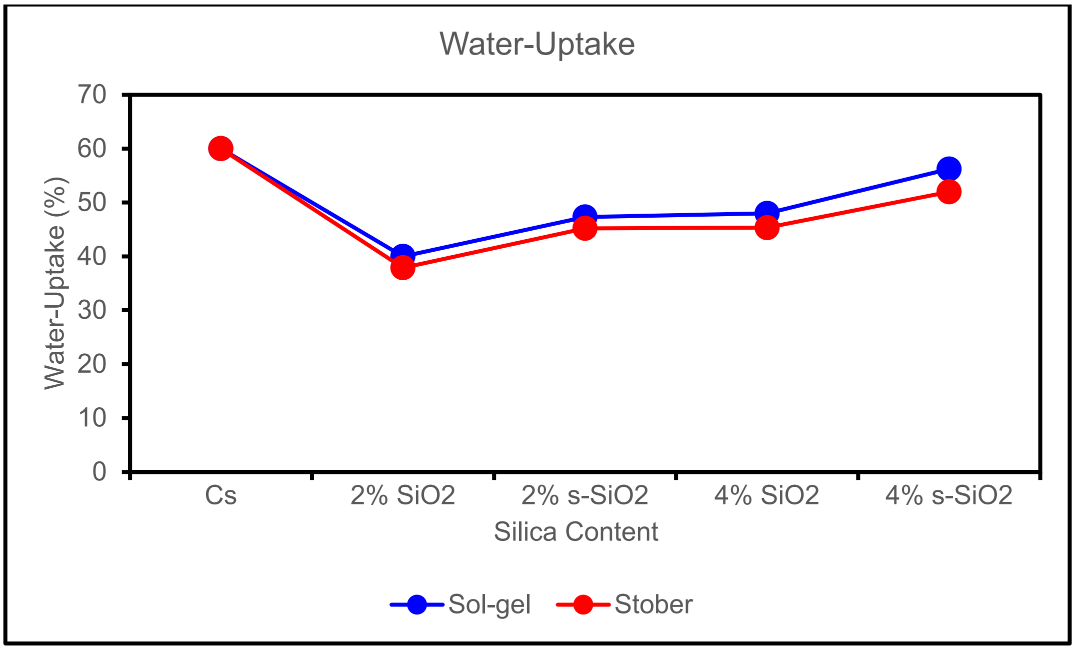

(**A**)

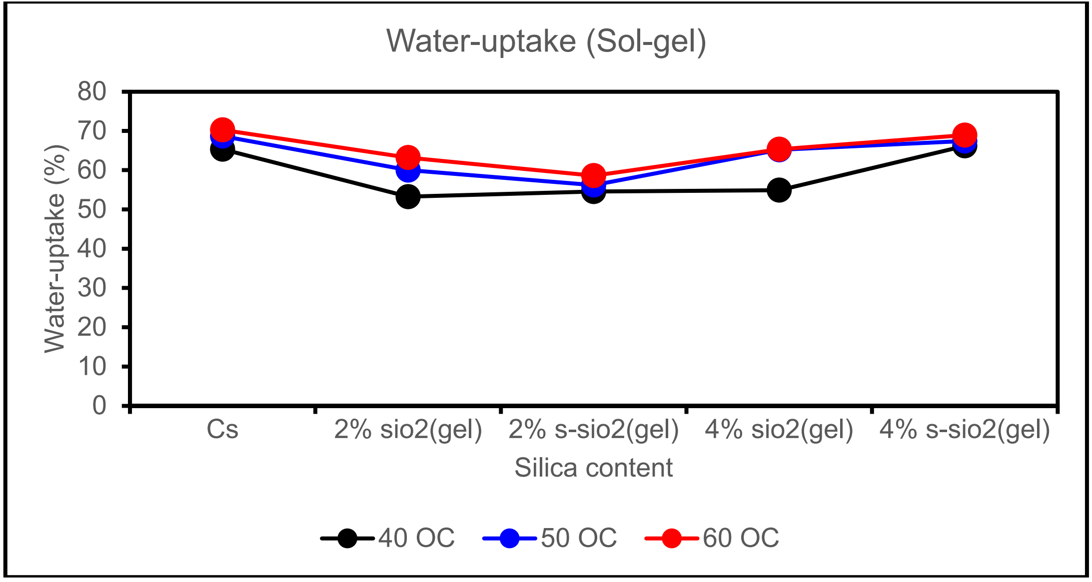

(**B**)

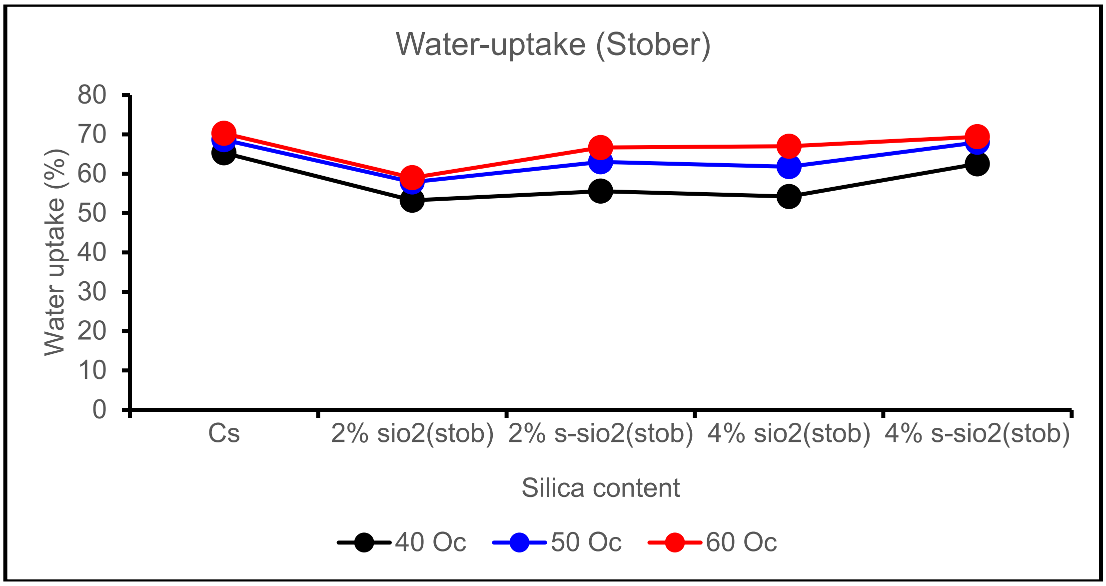

(**C**)

Figure 4. (**A**) Effect of silica content on water uptake of (a) Cs (b) 2% s-SiO_2/Cs (c) 2% SiO_2/Cs (d) 4% s-SiO_2/Cs (e) 4% SiO_2/Cs—**Sol-gel (2h)** and **Stober (2h)**. (**B**) Effect of temperature on water uptake of (a) Cs (b) 2% s-SiO_2/Cs (c) 2% SiO_2/Cs (d) 4% s-SiO_2/Cs (e) 4% SiO_2/Cs—**Sol-gel (2h)**. (**C**) Effect of temperature on water uptake of (a) Cs (b) 2% s-SiO_2/Cs (c) 2% SiO_2/Cs (d) 4% s-SiO_2/Cs (e) 4% SiO_2/Cs—**Stober (2h)**.

4.5. Ion Exchange Capacity of chitosan membranes

The ion exchange capacity of the membranes is illustrated in Figure 5. It is indicated in Figure 5 that pure chitosan has the lowest IEC of 0.77 meq/g and the addition of silica improves the chitosan membrane's IEC from 1.12 meq/g (2% SiO_2) to the highest exchange value of 2.32 meq/g (4% s-SiO_2). Sulfonated Sol-gel membranes have the highest IEC, and it is mainly due to the presence of acid groups caused by SiO_2-SO_3H particles' acidity. The overall results indicate that incorporating silica nanoparticles can boast superior ion exchange capacities compared to their chitosan counterpart. The increase in IEC can be attributed to (i) Chitosan having amino groups that can be deprotonated or protonated to allow for the exchange of ions (ii) the addition of functional groups in the chitosan layer that improves the site available for exchange [31] (iii) The incorporation of silica nanoparticles into chitosan membranes can improve the surface accessibility of certain functional groups and the silica's structure facilitates the movement of ions into the matrix, enhancing the exchange of ions (iv) The chemical and mechanical properties of chitosan-based membranes can be improved through the incorporation of silica which will extend their service life and improve their ability to exchange ions.

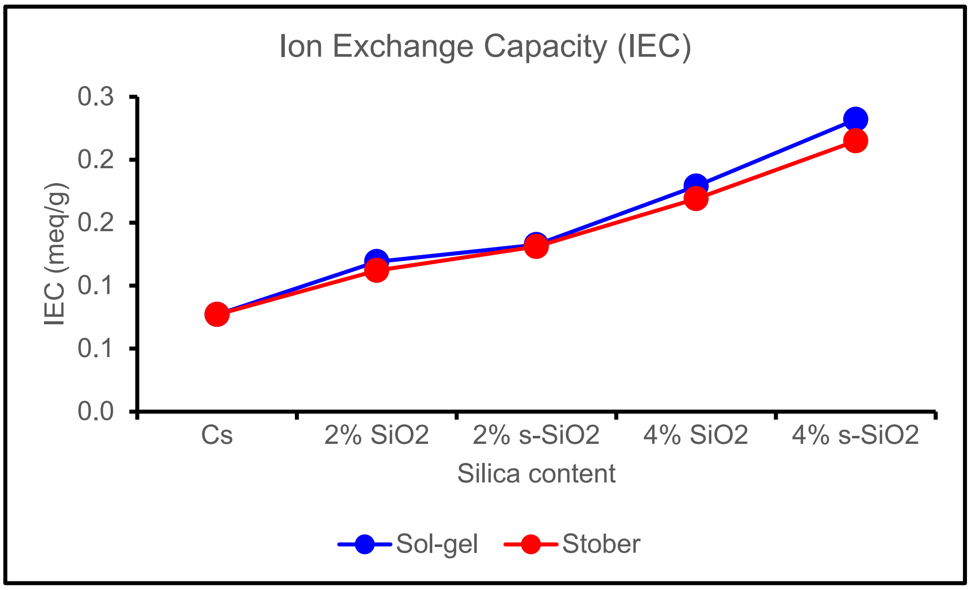

Figure 5. Ion exchange capacity of (a) Cs (b) 2% s-SiO_2/Cs (c) 2% SiO_2/Cs (d) 4% s-SiO_2/Cs (e) 4% SiO_2/Cs (i)-**Sol-gel (2h)** and **Stober (2h).**

4.6. Proton Conductivity of chitosan membranes

Figure 6 indicates the proton conductivity of the chitosan membrane at room temperature. The proton conductivity of the membrane is an important contributing factor in the application of membranes in fuel cells. It helps in determining if the membrane can produce the energy needed. The vehicle and the Grotthuss mechanisms are responsible for proton transfers in PEM [32]. In Figure 6 an increase in proton conductivity was observed when more filler was added, this is due to the influence of ionic groups Si-OH which facilitate proton conduction. Chitosan was reported to have a proton conductivity of 0.151 cm/s and that of modified membranes (2% SiO_2) having the lowest proton conductivity of 0.206 cm/s and 0.21 cm/s with the highest conductivity (4% s-SiO_2) 0.229 cm/s and 0.234 cm/s Stober and Sol-gel respectively. The high increase in proton conductivity of s-SiO_2 Sol-gel membranes can be attributed to the high-water uptake of the membranes reported in Figure 4. The proton conductivity of PEM is affected by the presence of water, as well as the dissociation of the groups of mobile protons and sulfonic groups therefore enhanced water uptake helps facilitate proton transfers through membranes' ionic channels [33]. The reason why the conductivity of the membranes is outstanding is due to the presence of high-proton-conducting sulfonating compounds that are stuck in the routes of the sulfonating polymers and SiO_2.

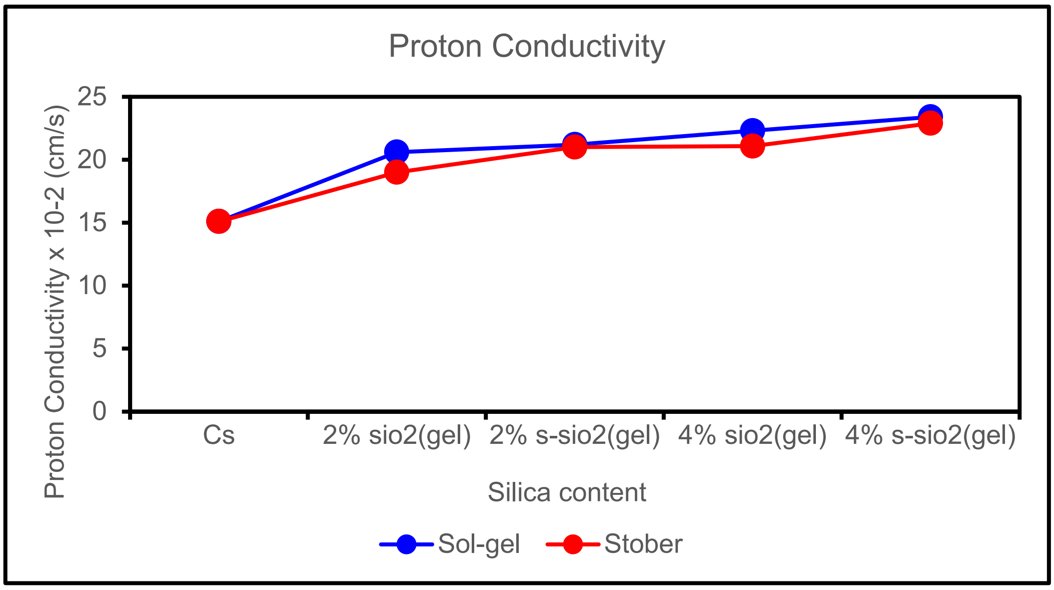

Figure 6. Proton conductivity of (a) Cs (b) 2% s-SiO_2/Cs (c) 2% SiO_2/Cs (d) 4% s-SiO_2/Cs (e) 4% SiO_2/Cs—**Sol-gel (2h)** and **Stober (2h)**.

4.7. Methanol Permeability of chitosan membranes

DMFCs are powered by methanol as fuel, and having low permeability of PEM will contribute to their efficiency. The effect of the silica particles' content on the Chitosan composite membranes' methanol permeability is shown in Figure 7, also Figure 7 shows the relationship between the time and permeability behaviour of a membrane. It indicates that with time, the chitosan membrane's permeability increases. It was also observed that adding silica nanoparticles can reduce the crossover between the membrane and methanol. The lowest methanol permeability on the modified membrane is found on a 4% s-SiO_2 membrane and its value is 0.99 x 10^{-7} cm^2/s at 30 minutes and 3.31 x 10^{-7} cm^2/s at 60 minutes on Sol-gel. The decrease in Permeability is due to ion-exchangeable acid groups that promote proton conduction by forming a hydrogen bond network that is strong enough to resist methanol permeability [34,35]. The permeability of the modified chitosan membrane decreases by almost 2 % when compared to the unmodified silica-chitosan material. This phenomenon is due to the cross-linked structure in the modified membranes. The Stober membranes have the lowest methanol permeability of 2.2 x 10^{-7} on a 4% s-SiO_2 membrane for the first 30 minutes. As time increases the methanol permeability on Stober membranes also increases to 3.39 x 10^{-7} and 3.57 x 10 $^{-7}$ on 2% SiO_2 and 4% s-SiO_2 membranes respectively.

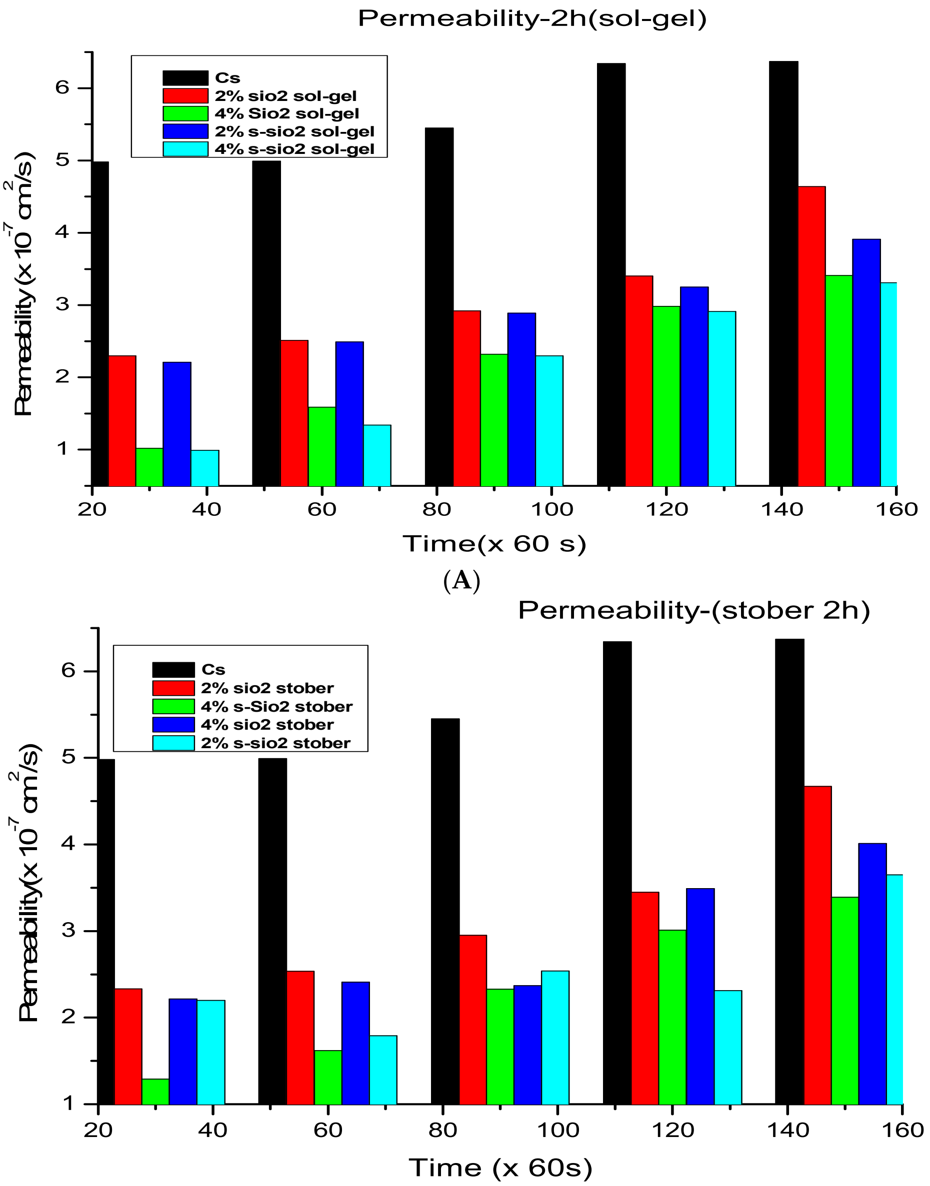

(**A**)

(**B**)

Figure 7. (**A**) Methanol permeability of (a) Cs (b) 2% s-SiO_2/Cs (c) 2% SiO_2/Cs (d) 4% s-SiO_2/Cs (e) 4% SiO_2/Cs—**Sol gel (2h)**. (**B**) Methanol permeability of (a) Cs (b) 2% s-SiO_2/Cs (c) 2% SiO_2/Cs (d) 4% s-SiO_2/Cs (e) 4% SiO_2/Cs—**Stober** (2h).

4.8. Tensile strength of chitosan membranes

The mechanical properties of chitosan membranes are shown in Figure 8. The results indicate that the strength of these membranes improved when 2% inorganic filler was added, but it then weakened when 4% was added. The chitosan membranes' tensile strength was 3.33 MPa before modification. When silica was added the tensile strength increased to 5.56 and 4.97 MPa. This was followed by a significant increase of 5.76 and 5.89 MPa when 2% s-SiO_2 Sol-gel and Stober were used respectively. This suggests that the sulfonation of these particles has a significant impact on the chitosan membranes' mechanical strength. An increase in the filler content to 4% resulted in a decline in its strength. The lowest value was 4% SiO_2 (4,32 MPa) Stober. This is consistent with the findings of a 2014 study by Narsito et al, who stated that high silica content can harden a membrane [36]. The membrane tensile strength in membranes with silica synthesized through Sol-gel and Stober processes have similar behaviour concerning the effect of silica on tensile strength. It can be concluded that the modification of silica with sulphur successfully improves the membrane's tensile

Preprints (www.preprints.org) | NOT PEER-REVIEWED | Posted: 17 July 2023 doi:10.20944/preprints202307.1088.v1

strength. However, it is also important to keep the quantity of silica incorporated into the membrane at a minimum as to strengthen its mechanical strength.

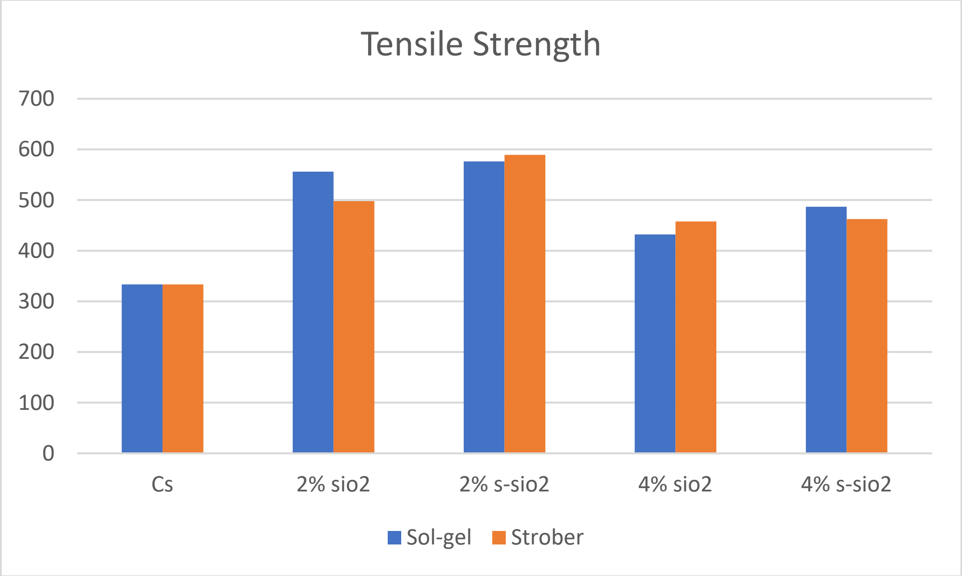

Figure 8.

5. Conclusion

The FTIR spectra show no chemical reactions between chitosan and modified silica particles. Instead, the physical interaction between the two occurs. As the elevated silica content increases, its favorable characteristics, such as water uptake and proton conductivity, increase while the methanol permeability decreased. This makes it an ideal material for fuel cells. The amount of water absorbed by chitosan membranes containing silica was observed to increase from 2 % to 4 % SiO_2. Silica-based membranes that have been calcined for two hours show an increase in water uptake from 37.9 % to 51.97 Stober and from 40 % to 56.21 % Sol-gel. Sulfonated membranes exhibited exceptional proton conductivities of 0.229 cm/s and 0.234 cm/s on 4 % Stober and Sol-gel respectively. Despite having a lower proton conductivity than membranes modified with sulfonated silica, pure silica-incorporated membranes had a greater proton conductivity than pure chitosan (0.151 S/cm). The reduction in methanol permeability was observed in developed membranes when silica was added from 2 % to 4 %. In conclusion, silica-modified chitosan membranes have enormous potential for use in direct methanol fuel cells (DMFC). The addition of silica to chitosan membranes has several benefits that improve their functionality and appropriateness for DMFCs. First, silica enhances the stability and mechanical strength of chitosan membranes. Under the demanding operating circumstances of DMFCs, silica particles support the chitosan matrix, preventing membrane deformation and maintaining structural integrity. The membranes' durability is increased by this mechanical robustness, which allows them to tolerate mechanical loads. The chitosan membranes with silica particles have better barrier properties against the flow of methanol, which is a critical issue when it comes to DMFCs. By minimizing the crossover between the fuel cell and the membrane, the modified membranes can help improve their efficiency and prevent it from running over the chemical. Furthermore, the addition of silica nanoparticles enhances proton conductivity in chitosan membranes. Silica acts as a proton conductor, facilitating the transport of protons across the membrane and improving the overall cell performance. This increased proton conductivity will contribute to higher power output and efficiency of the DMFC. Additionally, chitosan membrane proton conductivity was improved by the addition of silica nanoparticles, and proton transport across the membrane was made easier by the role of silica as a proton conductor, which enhances cell function in general. The improvement in proton conductivity and methanol permeability makes the fabricated membranes suitable for applications in fuel cells. It can be concluded that the modification of chitosan with modified silica is necessary to improve the suitability of chitosan in fuel cell technology. Although membrane membranes modified with sulfonated silica show exceptional results in terms of proton conductivity, water uptake is a challenge that still needs to be addressed. However, fuel cell performance must also be done to support the reliability of the fabricated membranes in fuel cells. Optimizing the synthesis processes and exploring the full potential of chitosan membranes modified with silica for DMFC applications still require additional research and development, it is crucial.

References

1. Bayrak ZU, Gencoglu MT. Application areas of fuel cells. In: *Proceedings of 2013 International Conference on Renewable Energy Research and Applications, ICRERA 2013*. IEEE Computer Society; 2013:452-457. doi:10.1109/ICRERA.2013.6749798
2. Kasyanova A V., Zvonareva IA, Tarasova NA, Bi L, Medvedev DA, Shao Z. Electrolyte materials for protonic ceramic electrochemical cells: Main limitations and potential solutions. *Mater Reports Energy*. 2022;2(4):100158. doi:10.1016/j.matre.2022.100158
3. Halim FA, Hasran UA, Masdar MS, Kamarudin SK, Daud WRW. Overview on Vapor Feed Direct Methanol Fuel Cell. *APCBEE Procedia*. 2012;3:40-45. doi:10.1016/j.apcbee.2012.06.043
4. Vaghari H, Jafarizadeh-Malmiri H, Berenjian A, Anarjan N. Recent advances in application of chitosan in fuel cells. *Sustain Chem Process*. 2013;1(1):1. doi:10.1186/2043-7129-1-16
5. Qussay R, Mahmood M, Al-Zaidi MK, Al-Khafaji RQ, Al-Zubaidy DK, Salman MM. A Review: Fuel Cells Types and their Applications. *Int J Sci Eng Appl Sci*. 2021;(7):2395-3470. www.ijseas.com
6. Ebrahimi M, Kujawski W, Fatyeyeva K, Kujawa J. A review on ionic liquids-based membranes for middle and high temperature polymer electrolyte membrane fuel cells (Pem fcs). *Int J Mol Sci*. 2021;22(11). doi:10.3390/ijms22115430
7. Ramadhani F, Hussain MA, Mokhlis H. A comprehensive review and technical guideline for optimal design and operations of fuel cell-based cogeneration systems. *Processes*. 2019;7(12). doi:10.3390/pr7120950
8. Tellez-Cruz MM, Escorihuela J, Solorza-Feria O, Compañ V. Proton exchange membrane fuel cells (Pemfcs): Advances and challenges. *Polymers (Basel)*. 2021;13(18):1-54. doi:10.3390/polym13183064
9. Olabi AG, Wilberforce T, Alanazi A, et al. *Novel Trends in Proton Exchange Membrane Fuel Cells*. Vol 15.; 2022. doi:10.3390/en15144949
10. Ohashi M. *Direct Methanol Fuel Cell as the next Generation Power Source*.
11. Baruah B, Deb P. Performance and application of carbon-based electrocatalysts in direct methanol fuel cell. *Mater Adv*. 2021;2(16):5344-5364. doi:10.1039/d1ma00503k
12. Ahmed AA, Al Labadidi M, Hamada AT, Orhan MF. Design and Utilization of a Direct Methanol Fuel Cell. *Membranes (Basel)*. 2022;12(12). doi:10.3390/membranes12121266
13. Off-grid Photovoltaic system with Battery Storage and Direct Methanol Fuel Cell as a. 2020;(January):0-10. doi:10.13140/RG.2.2.12494.82240
14. Chou CJ, Jiang SB, Yeh TL, Tsai LD, Kang KY, Liu CJ. A portable direct methanol fuel cell power station for long-term internet of things applications. *Energies*. 2020;13(14). doi:10.3390/en13143547
15. Goor M, Menkin S, Peled E. High power direct methanol fuel cell for mobility and portable applications. *Int J Hydrogen Energy*. 2019;44(5):3138-3143. doi:10.1016/j.ijhydene.2018.12.019
16. Kamarudin SK, Achmad F, Daud WRW. Overview on the application of direct methanol fuel cell (DMFC) for portable electronic devices. *Int J Hydrogen Energy*. 2009;34(16):6902-6916. doi:10.1016/j.ijhydene.2009.06.013
17. Ghouse M. Fuel Cells and Their Applications Prof . M . Ghouse King Abdulaziz City for Science and Technology (KACST) Riyadh , Saudi Arabia 17 th June 2012. 2016;(June 2012). doi:10.13140/RG.2.1.2579.0482
18. Kartika Sari A, Mohamad Yunus R, Majlan EH, et al. Nata de Cassava Type of Bacterial Cellulose Doped with Phosphoric Acid as a Proton Exchange Membrane. *Membranes (Basel)*. 2023;13(1). doi:10.3390/membranes13010043
19. Selim A, Szijjártó GP, Tompos A. Insights into the Influence of Different Pre-Treatments on Physicochemical Properties of Nafion XL Membrane and Fuel Cell Performance. *Polymers (Basel)*. 2022;14(16). doi:10.3390/polym14163385

20. Sherazi TA, Guiver MD, Kingston D, Ahmad S, Kashmiri MA, Xue X. Radiation-grafted membranes based on polyethylene for direct methanol fuel cells. *J Power Sources*. 2010;195(1):21-29. doi:10.1016/j.jpowsour.2009.07.021
21. Hwang S, Lee HG, Jeong YG, et al. Polymer Electrolyte Membranes Containing Functionalized Organic/Inorganic Composite for Polymer Electrolyte Membrane Fuel Cell Applications. *Int J Mol Sci*. 2022;23(22). doi:10.3390/ijms232214252
22. Kabir Chowdury MS, Cho YJ, Park SB, Park Y il. Review—Functionalized Graphene Oxide Membranes as Electrolytes. *J Electrochem Soc*. Published online 2023. doi:10.1149/1945-7111/acc35e
23. Adiyar SR, Satriyatama A, Azjuba AN, Sari NKAK. An overview of synthetic polymer-based membrane modified with chitosan for direct methanol fuel cell application. *IOP Conf Ser Mater Sci Eng*. 2021;1143(1):012002. doi:10.1088/1757-899x/1143/1/012002
24. Fatullayeva S, Tagiyev D, Zeynalov N, Mammadova S, Aliyeva E. Recent advances of chitosan-based polymers in biomedical applications and environmental protection. *J Polym Res*. 2022;29(7). doi:10.1007/s10965-022-03121-3
25. Junoh H, Jaafar J, Nik Abdul NAH, et al. Performance of polymer electrolyte membrane for direct methanol fuel cell application: Perspective on morphological structure. *Membranes (Basel)*. 2020;10(3). doi:10.3390/membranes10030034
26. Peyrovi MH, Parizi MA. The Modification of the BET Surface Area by Considering the Excluded Area of Adsorbed Molecules. *Phys Chem Res*. 2022;10(2):173-177. doi:10.22036/pcr.2021.290859.1924
27. Brunauer_Emmett_Teller_BET_Theory.
28. Bunaciu AA, Udriştioiu E gabriela, Aboul-Enein HY. X-Ray Diffraction: Instrumentation and Applications. *Crit Rev Anal Chem*. 2015;45(4):289-299. doi:10.1080/10408347.2014.949616
29. Lee EJ, Shin DS, Kim HE, Kim HW, Koh YH, Jang JH. Membrane of hybrid chitosan-silica xerogel for guided bone regeneration. *Biomaterials*. 2009;30(5):743-750. doi:10.1016/j.biomaterials.2008.10.025
30. Nur Y, Rohaeti E, Darusman LK. Optical sensor for the determination of Pb2+ based on immobilization of dithizone onto Chitosan-Silica membrane. *Indones J Chem*. 2017;17(1):7-14. doi:10.22146/ijc.23560
31. Purwanto M, Widiastuti N, Saga BH, Gusmawan H. Synthesis of Composite Membrane Based Biopolymer Chitosan with Silica from Rice Husk Ash for Direct Methanol Fuel Cell Application. *IOP Conf Ser Earth Environ Sci*. 2021;830(1). doi:10.1088/1755-1315/830/1/012021
32. Zuo Z, Fu Y, Manthiram A. Novel blend membranes based on acid-base interactions for fuel cells. *Polymers (Basel)*. 2012;4(4):1627-1644. doi:10.3390/polym4041627
33. Bai H, Zhang H, He Y, Liu J, Zhang B, Wang J. Enhanced proton conduction of chitosan membrane enabled by halloysite nanotubes bearing sulfonate polyelectrolyte brushes. *J Memb Sci*. 2014;454:220-232. doi:10.1016/j.memsci.2013.12.005
34. Kusumastuti E, Siniwi WT, Mahatmanti FW, Jumaeri J, Atmaja L, Widiastuti N. Modification of chitosan membranes with nanosilica particles as polymer electrolyte membranes. *AIP Conf Proc*. 2016;1725(April 2016). doi:10.1063/1.4945491
35. Lue SJ, Pai YL, Shih CM, Wu MC, Lai SM. Novel bilayer well-aligned Nafion/graphene oxide composite membranes prepared using spin coating method for direct liquid fuel cells. *J Memb Sci*. 2015;493:212-223. doi:10.1016/j.memsci.2015.07.007
36. Widhi Mahatmanti F, Nuryono, Narsito. Physical characteristics of chitosan based film modified with silica and polyethylene glycol. *Indones J Chem*. 2014;14(2):131-137. doi:10.22146/ijc.21249